A QUANTUM DEVICE SIMULATOR BASED ON THE NON-EQUILIBRIUM GREEN FUNCTION EQUATIONS OF KELDYSH, KADANOFF, AND BAYM

Roger Lake, Gerhard Klimeck, Michael McLennan[1], and Supriyo Datta
School of Electrical Engineering, Purdue University West Lafayette, IN 47907

Abstract

Simulation of high-bias quantum electron transport with inelastic scattering is described. With all energies coupled by inelastic processes and current flowing at energies above and below the incident energy, optimization of the energy grid becomes crucial. The optimization method is described and examples are given.

1. Introduction

The modeling of high bias quantum electron transport with inelastic scattering is challenging. The coupling of all energies necessitates the resolution of an energy range comparable to that of the applied bias. In a Tsu-Esaki tunneling formula [1], only the energy range of the incident electrons in the contacts needs to be considered. Within the broad energy range of the applied bias, resonances in the spectral function on the order of 0.1 meV along with their phonon echoes must be well resolved to obtain a correct, current-conserving solution.

Our approach is based on the many-body, non-equilibrium theory of Keldysh, Kadanoff, and Baym (KKB) [2,3] which is a field-theoretic description of the many-particle Schrödinger equation. It is fundamental, general, and allows a diagrammatic perturbation treatment of the electron-phonon interaction. Furthermore, the Pauli exclusion principle is built into the formalism. We directly solve, in steady-state, the coupled non-equilibrium Green function equations as described in [4].

2. Model

The model that we solve numerically consists of a single particle Hamiltonian, $H_o=\mathbf{p}^2/2m^*+V(\mathbf{r})$, a phonon bath maintained in thermodynamic equilibrium, $H_B = \sum_m \hbar\omega_m(a_m^\dagger a_m + 1/2)$, and the electron-phonon interaction $H' = \sum_m U\delta(\mathbf{r}-\mathbf{r}_m)(a_m^\dagger + a_m)$. The interaction is local in space. In the expression for H', the sum over m becomes an integral, $\Sigma_m \rightarrow \int d\mathbf{r}\int dE\, J_0(\mathbf{r};E)$ where J_0 is the density of phonon modes. The position dependence of J_0 is uniform; phonon scattering is present throughout our system, from $-\infty$ to $+\infty$. We use two different spectra, $J_0(E)$, and corresponding strengths, U: a Debye spectrum $\sim \omega^2\theta(\omega_D-|\omega|)$ where $\hbar\omega_D=20$ meV and an Einstein spectrum $\sim \delta(\omega\pm\omega_0)$ where $\hbar\omega_o=36$ meV. When the Einstein spectrum is used, our model for the interaction, is equivalent to $H_{ep}(\mathbf{r},t) = V^{-1/2} M \sum_{\mathbf{q}} e^{i\mathbf{q}\cdot\mathbf{r}}(a_{\mathbf{q}}e^{-i\omega_o t} + a_{-\mathbf{q}}^\dagger e^{i\omega_o t})$.

3. Formalism

The formalism, which is discussed in detail in refs. [4,5], begins with the steady-state equations for the retarded Green function, G^R, and the correlation function, $G^<$, which we write in matrix notation.

$$(E - H_o - \Sigma^R)\, G^R = 1 \tag{3.1}$$

and

$$(E - H_o - \Sigma^R)\, G^< = \Sigma^< G^{R\dagger} \tag{3.2}$$

In the position representation, the representation in which we work, equations (3.1) and (3.2) are linear integro-differential equations in the position coordinate. G^R is the impulse response for the operator on the left-hand side of eq. (3.2). Furthermore, since we have damping from the electron-phonon interaction throughout our system, G^R satisfies the same boundary conditions as $G^<$, namely $G^R(\mathbf{r},\mathbf{r}';E) \underset{\mathbf{r}-\mathbf{r}'\rightarrow\infty}{\rightarrow} 0$. Thus, the solution to (3.2) can immediately be written as

$$G^< = G^R \Sigma^< G^{R\dagger} \tag{3.3}$$

Equations (3.1) and (3.3) along with the equations for the self-energies are the ones that we solve numerically. Since our model for the electron-phonon interaction is local, the self-energies are local. We define the scattering times, τ_n, τ_p, and τ_ϕ, via the following definitions.

$\Sigma^<(r_1,r_2;E) = -i\hbar/\tau_p(r_1;E)\,\delta(r_1-r_2)$, $\Sigma^>(r_1,r_2;E) = +i\hbar/\tau_n(r_1;E)\,\delta(r_1-r_2)$, and $\Sigma^R(r_1,r_2;E) = [\sigma(r_1;E) - i\hbar/2\tau_\phi(r_1;E)]\,\delta(r_1-r_2)$ where, following the discussion of Kadanoff and Baym [3], we associate $1/\tau_n$ with the electron outscattering rate, $1/\tau_p$ with the hole outscattering rate, and $1/\tau_\phi$ with the total de-phasing rate. σ is the real part of Σ^R. We treat the electron-phonon interaction in the self-consistent first Born approximation, ie. the re-normalized Green functions are used for calculating the self-energies. Self-consistency is necessary to conserve current [4,6-8]. We ignore the real part of the retarded self energy. This does not affect current conservation. The real part only re-normalizes the energies. The imaginary or anti-Hermitian part is responsible for loss.

The expressions for the rates $1/\tau_n$ and $1/\tau_p$ have forms identical to Fermi's Golden Rule. The difference is that the density of states is calculated self-consistently with the scattering from the imaginary part of the retarded Green function. The expressions are

$$\frac{1}{\tau_p(r;E)} = \frac{2\pi}{\hbar}\int d(\hbar\omega)\, F(\hbar\omega)\, N_0(r;E-\hbar\omega)\, f(r;E-\hbar\omega) \tag{3.4a}$$

$$\frac{1}{\tau_n(r;E)} = \frac{2\pi}{\hbar}\int d(\hbar\omega)\, F(\hbar\omega)\, N_0(r;E+\hbar\omega)\,[\,1-f(r;E+\hbar\omega)\,] \tag{3.4b}$$

where $N_0(r;E)$ is the electron density of states $(-1/\pi\,\mathrm{Im}G^R(r,r;E))$, $f(r;E)$ is the non-equilibrium occupation of N_0, ie.

$$f(r;E)\,N_o(r;E) \doteq G^<(r,r;E)/2\pi \tag{3.5}$$

and

$$F(E) = U^2 J_o(|E|)\begin{cases} N(E) & , E>0 \\ N(|E|+1 & , E<0 \end{cases} \tag{3.6}$$

In (3.6), J_o is the phonon spectrum, Debye or Einstein, U is a constant strength, and N is the Bose-Einstein factor. The total scattering rate is

$$\frac{1}{\tau_\phi(r;E)} = \frac{1}{\tau_n(r;E)} + \frac{1}{\tau_p(r;E)} \tag{3.7}$$

If the Einstein spectrum is used in (3.4), the rates, $\frac{1}{\tau_{p(n)}}$ take a particularly simple form.

$$\frac{1}{\tau_n(E)} = \frac{2\pi}{\hbar}U^2\,[\,N(\omega_0)+\frac{1}{2}\mp\frac{1}{2}\,]\,N_0(E\pm\hbar\omega_0)\,[\,1-f(E\pm\hbar\omega_0)\,] \tag{3.8a}$$

$$\frac{1}{\tau_p(E)} = \frac{2\pi}{\hbar}U^2\,[\,N(\omega_0)+\frac{1}{2}\mp\frac{1}{2}\,]\,N_0(E\mp\hbar\omega_0)\,f(E\mp\hbar\omega_0) \tag{3.8b}$$

In (3.8), the position coordinate has been suppressed and the upper (lower) sign corresponds to absorption (emission).

Using (3.5), (3.3) can be re-written for $f(r;E)$.

$$f(r;E) = \frac{1}{N_0(r;E)}\,\frac{\hbar}{2\pi}\int dr'\,\frac{|G^R(r,r';E)|^2}{\tau_p(r';E)} \tag{3.9}$$

Substituting (3.4a) into (3.9) results in a homogeneous integral equation in space and energy for the non-equilibrium occupation factor, $f(r;E)$.

$$f(r;E) = \frac{1}{N_o(r;E)}\int dr'\int dE'\,|G^R(r,r';E)|^2\,F(r',E')\,N_o(r';E-E')\,f(r';E-E') \tag{3.10}$$

The spatial boundary condition on (3.10), which gives the inhomogeneous term, is that $f(r;E)$ is the Fermi-Dirac factor in the contacts.

Equations (3.1), (3.4), (3.7), and (3.9) are solved iteratively. After convergence, $G^<(r,r';E)$ can be calculated from (3.3) and the current density is then found from

$$J(r;E) = \frac{-c\hbar}{4\pi m^*} \lim_{r'\to r} [\,(\nabla-\nabla')G^<(r,r';E)\,] \tag{3.11}$$

4. Numerical Implementation, Current Conservation, and the Energy Grid

Mesoscopic structures, such as a DBRTD, have narrow resonances on the order of a few tenths meV that need to be well resolved. Under high bias such that the Fermi-energies of the contacts are split by many K_BT, and with inelastic scattering, the current from the emitter flows through the device at energies above and below the injection energies. A good energy grid is essential to obtaining the correct, current-conserving solution.

The quantities which need to be resolved in energy are the following: (1) the density of states (resonances), (2) $\partial f/\partial E$ in the contacts - the sharp cut-off at the Fermi-energy at low temperatures, (3) the scattering rate, $1/\tau_\phi$, and (4) the current density per unit energy, J(z;E). The scattering rate, $1/\tau_\phi$, is a functional of the density of states, $N_o(z;E)$, and their occupation, f(z;E). For Einstein phonons, the relation is given by (3.8). The scattering rate at energy E is determined by $N_0(E\pm\hbar\omega_o)$ and $f(E\pm\hbar\omega_o)$. Also, since $N_0 = -1/\pi\,\mathrm{Im}G^R(z,z;E)$ is calculated self-consistently with τ_ϕ, N_o will be enhanced at each $n\hbar\omega_o$ above and below a resonance, $E_R \pm \hbar\omega_o$. The enhancement dies off exponentially with n, and for realistic scattering times, 0.1 - 1.0 ps, we have only seen echo peaks in N_o at $E_R \pm \hbar\omega_o$. In such instances we see enhancements in $1/\tau_\phi$ at one and two $\hbar\omega_o$ above and below the resonance. Thus, the resonant energy plus one and two optical phonon energies above and below the resonance must be finely resolved. If the energy grid is well resolved for the above quantities, then it will generally be well resolved for the energies at which the current is flowing since the majority of the current will be flowing through the main resonance or one or two $\hbar\omega_o$ above or below the main resonance. However, if the current is flowing off resonance, then we need to resolve the energies of the Fermi-sea in the emitter and energies several $\hbar\omega_o$ above and below the energies of the emitter Fermi sea.

The optimization of the energy grid begins with a Romberg integration of $N_0(z;E)$ to create a monotonically increasing function of energy, M(z;E).

$$M(z;E) = \int_{E_{min}}^{E} dE'\, N_0(z;E') \tag{4.1}$$

A constant value for τ_ϕ of ~0.1–1.0 ps is used when evaluating $G^R(z,z;E)$. Thus, the N_0 that is integrated contains the main resonances but not the phonon echoes. A second function, $M_N(z;E)$, is created

$$M_N(z;E) = M(z;E) + \alpha_1 M(z;E-\hbar\omega_o) + \alpha_2 M(z;E+\hbar\omega_o) + \alpha_3 M(z;E-2\hbar\omega_o) + \alpha_4 M(z;E+2\hbar\omega_o) \tag{4.2}$$

where α_x are scaling factors < 1. A third monotonically increasing function of energy is created, $M_f(z;E)$, defined by

$$M_f(z;E) = \int_{E_{min}}^{E} dE'\,(-\partial f(z;E')/\partial E') \tag{4.3}$$

M_f and M_N are normalized to their maximum values, weighted, added, and integrated over position to form the function that is used to optimize the energy grid, $M_{opt}(E)$.

$$M_{opt}(E) = \int dz\, M_f(z;E) + \sum_i \int_{R_i} dz\, c_1\, M_N(z;E) \tag{4.4}$$

where R_i represents user specified spatial regions of integration. The vertical M_{opt} axis is divided into equally spaced nodes whose number corresponds to the desired number of energy grid points. The nodes are projected horizontally across to the function $M_{opt}(E)$ and then vertically down to the energy axis. The intersections with the energy axis are the optimized energy grid points. If necessary, after several iterations, a similar type of optimization can be done based on the energy distribution of the current density.

5. Numerical Examples

Two examples are shown where the current is flowing not only at the incident energy but at one or more optical phonon energies below the injection energy. The first is from a simulation of a DBRTD at 4.2K biased such that the incident electrons are tunneling into the well one optical phonon energy above

the resonant energy. They emit optical phonons in the well and in Fig. 1a, approximately 1/2 of the incident electrons scatter down to the resonance. Current leaves the well both at the incident energy and at the resonant energy. Fig. 1b shows the density of states in the well with an echo of the resonance at $E_R + \hbar\omega_o$. Fig. 2a shows the density of states for a superlattice beginning to form a miniband, and Fig. 2b shows the energy distribution of the current flowing through the miniband. The three bands of current flowing beneath the energy of the incident current are each spaced $\hbar\omega_o$ apart.

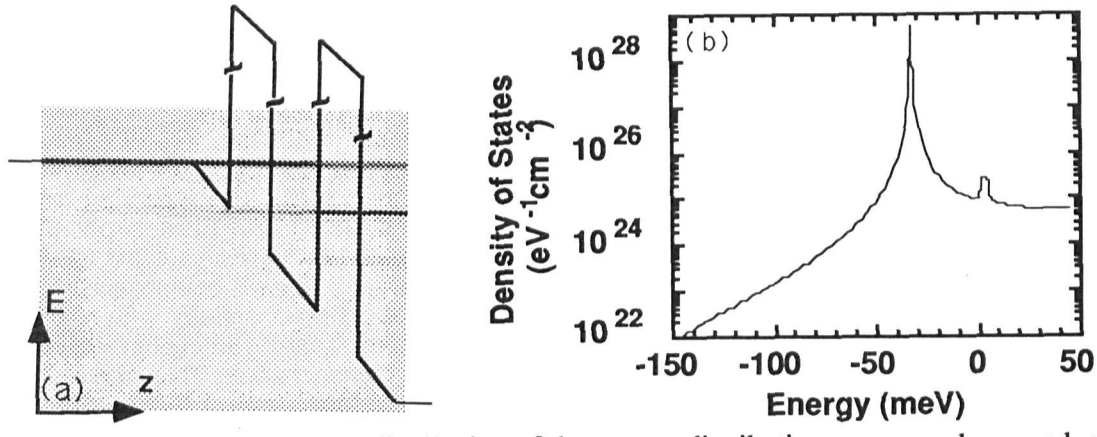

Fig. 1. (a) Gray scale plot of energy distribution of the current distribution superposed on conduction band profile. (b) Spectral function in well.

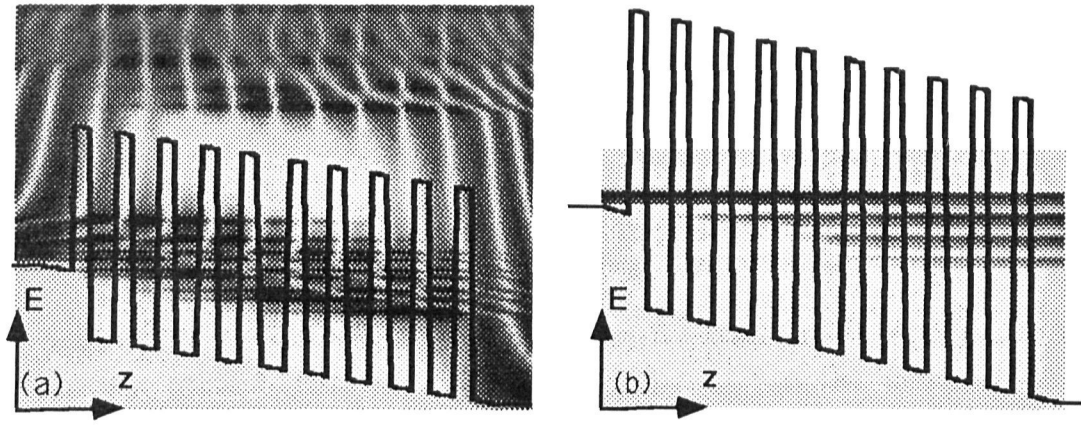

Fig. 2. (a) Density of states of a superlattice. (b) Current flow through the superlattice.

Acknowledgement
This work was supported by the Semiconductor Research Corporation under contract no. 91-SJ-089.
[1]Present address: AT&T Bell Laboratories, Allentown, PA.

References

1. R. Tsu and L. Esaki, *Appl. Phys. Lett.*, **22**, 562 (1973).
2. L.V. Keldysh, *Zh. Eksp. Teor. Fiz.*, **47**, 1515 (1964). [Sov. Phys. JETP **20**, 1018, (1965)].
3. L.P. Kadanoff and G. Baym, *Quantum Statistical Mechanics*, Benjamin, Reading MA, (1962).
4. R. Lake and S. Datta, *Phys. Rev. B*, **45**, 6670 (1992).
5. S. Datta, *J. Phys. Condens. Matter*, **2**, 8023 (1990).
6. P. Danielewicz, *Annals of Physics*, **152**, 239 (1984).
7. F.S. Khan, J.H. Davies, and J.W. Wilkins, *Phys. Rev. B*, **36**, 2578 (1987).
8. G.D. Mahan, *Physics Reports*, **145**, 251 (1987).